Pramana – J. Phys. (2022) 96:63
https://doi.org/10.1007/s12043-022-02306-1

Effects of mass and size of sand grains on the physical properties of eroded glass

A FACI[1], S BENTERKI[1], M FATMI[2],*, SAMEH I AHMED[3] and B BARKA[2]

[1]Laboratory of Nonmetallic Materials, Institute of Optics and Precision Mechanics, Ferhat Abbas University-Setif1, 19000 Sétif, Algeria
[2]Research Unit on Emerging Materials (RUEM), Ferhat Abbas University-Setif1, Sétif 19000, Algeria
[3]Department of Physics, College of Science, Taif University, P.O. Box 11099, Taif 21944, Saudi Arabia
*Corresponding author. E-mail: fatmimessaoud@yahoo.fr, m.fatmi@univ-sctif.dz

MS received 15 March 2021; revised 24 October 2021; accepted 9 November 2021

Abstract. We presented in this work the effect of sand mass and grains size on optical transmission and mechanical resistance of soda-lime glass subjected to sandblasting simulated in laboratory. Glass samples were sandblasted under various test conditions (projected sand masses M_p: from 5 to 120 g and grains size Φ: (300 ± 50, 1000 ± 114 and 1700 ± 175) μm). The results indicate that the size and density of defects increase when grain sizes and projected masses are enhanced, and the surface becomes more damaged. As the mass and size of the sand grains increase, the roughness and surface damage increase and reach the values of 41.2 μm and 52.7%, while for the most severe conditions ($M_p = 120$ g, $\Phi = 1700\,\mu$m), the maximum of the sizes of the defects generated on the sample surface is about 468 μm and the mechanical bending strength and optical transmission decrease significantly and reach the values of 9, 56 MPa and 12, 24%, respectively. The microscopic observations confirm our interpretations.

Keywords. Glass; sandblasting; surface damage; transmission; mechanical properties.

PACS Nos 61.43.Fs; 64.70.kj; 66.30.hh

1. Introduction

Erosion is a major problem because it destroys fragile materials. Erosion is a surface phenomenon associated with the removal of material by repeated impacts of solid particles. During sandstorms, the impact induced by particles on the surface of glass causes more or less serious damage [1,2]. Erosion is considered to be of elastoplastic type. The in-depth understanding of the cracking generated by erosion, the relationship between the relevant parameters involved in the erosion process and surface damage, such as the speed of impact, the projected mass, the size and the shape of grains of sand have been studied [3,4]. These factors are responsible for the kinetic energy of the incident particles. This energy considerably reduces the breaking strength and the optical transmission by scattering of incident light [5,6]. Many researchers have reported that the optical and mechanical properties are enormously affected by the microstructural defects in the glass [7–9]. For appropriate applications of these glasses, the electrical, thermal, mechanical and optical properties have been widely studied by many [10,11]. The reduction of light transmittance to a level (70–75)% significantly affects the driver's visual perception. Rompe and Engel [12] reported that the low transmittance of the windshield caused by wear has a detrimental effect on visibility. According to various parameters, which affect the erosion mechanism, several researchers based their works on the most relevant erosion kinetic energy of the incident particles, the projected mass and grain size. However, kinetic energy is the most relevant parameter to explain glass damage [13,14]. For example, kinetic energy of 100 J produces a surface defect of 1 cm^2 area and 1 mm depth. The surface defects are complex according to their diversity of shape, velocities and impact angles. The parameters quoted below are governed by the turbulence of the wind recorded at the ground level. The presence of dunes with variable sizes leads to random blasts of wind. It is difficult to study the effect of all these parameters on glass properties. Many researchers, in their studies, have chosen sizes of erosive particles generally less than 500 microns. In this work, we chose the projected mass and three sizes of

Published online: 24 March 2022

sand grains (fine, medium and large), Φ: (300 ± 50, 1000 ± 114 and 1700 ± 175) μm, which present the real conditions in Sahara, to study their effect on optical transmission and mechanical strength of a soda-lime sand glass. This choice accords well with the well-known mechanism of saltation in the phenomenon of erosion due to sandstorms.

2. Experimental procedure

2.1 *Experimental sandblasting conditions*

We used a sand blower apparatus for erosion tests. This is a horizontal jet impingement system recommended by the standards for airborne particle erosion testing (DIN 50 33218 and ASTM G761920) (ASTM, 1992; DIN, 1984) [15]. The samples were eroded with various sand masses (M_p = 5, 10, 20, 30, 40, 50, 70, 100 and 120 g) to obtain diverse surface states. According to the Ouargla weather service, the strongest storm recorded in this region reaches an average speed of 35 m s^{-1}. Since we based our study on the damage of glass in the most unfavourable case, we chose the speed of 25 m s^{-1} which is considered as a high speed in ordinary conditions (not exceptional) in the Ouargla region. The glass samples were positioned perpendicular to the sand flow ($\alpha = 90°$). We reported the following test conditions: The distance between the nozzle and the specimens x = 50 mm, diameter of the tube d = 25 mm and constant sand feed rate = 7.5 g.min^{-1} during all the erosion tests.

2.2 *Glass and sand*

We used a common silica-soda-lime glass manufactured by the company AfricaVer (Algeria) and has a sheet form with a thickness of 3 mm. The mean chemical composition and physical characteristics of silica-soda-lime glass are listed in tables 1 and 2. We synthesised square samples with 50 × 50 mm^2 dimensions from the same glass sheet. All these samples are sandblasted on the same side. The eroding material used in this study is the sand of the Aïn Aminas region (Southern Algeria). The chemical compositions of this sand are mainly quartz, tourmaline, limonite, gibbsite and some impurities. The shape of the particle is irregular and varies from nearly spherical to angular as shown in figure 1.

Table 1. Mean chemical composition of the glass used in this study.

Oxides	SiO_2	CaO	Na_2O	MgO	Al_2O_3	Fe_2O_3	Others
Mass (%)	71.56	7.92	13.73	4.21	1.32	0.097	1.163

Table 2. Some physical properties of glass.

Properties	Values
Thermal dilatation coefficient α	8.5×10^{-6} K^{-1}
Young modulus E	72.2 GPa
Poisson's coefficient υ	0.22
Density ρ	2.47 g cm^{-3}
Bending fracture strength	117 ± 23 MPa
Hardness	5.62 GPa
Optical transmission	91.5%

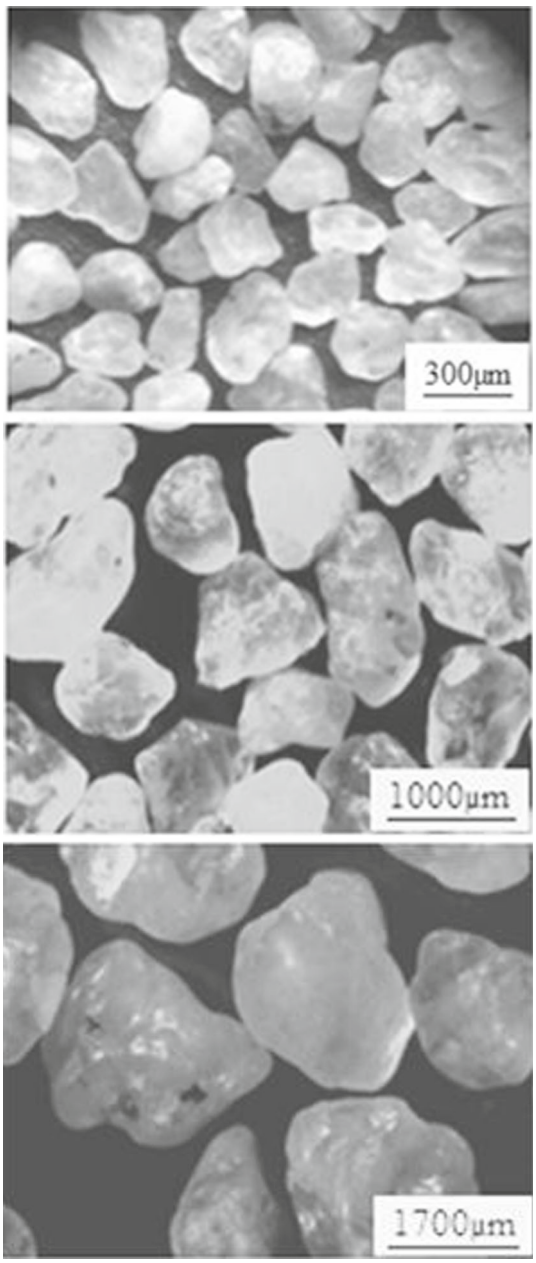

Figure 1. Optical micrograph showing a sample of sand grains with irregular shape.

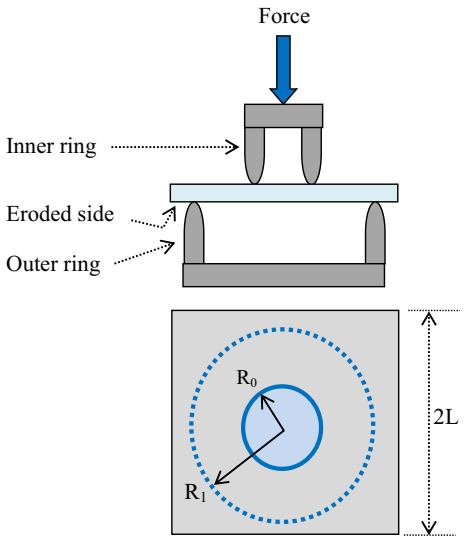

Figure 2. Schema of bending test using concentric rings.

2.3 *Mechanical characterisation*

The strength characterisation was done by concentric biaxial bending tests as illustrated in figure 2. This technique presents a major advantage in comparison to the three- and four-points device. This method essentially avoids the edge flaws and therefore determines the intrinsic strength. For these tests, sets of 30 samples of the same size ($50 \times 50\,\text{mm}^2$) were prepared for each sand mass and grains size erosion parameter. In concordance with ASTM C1499 recommendations [16], the device used in this study is composed of inner and outer rings having 16 mm and 36 mm diameter, respectively. According to Faci *et al* [17], the radius of the outer ring must be equal to; at least, six times the thickness of the tested sample. We placed the eroded surface on the tensile side during resistance tests. The loading speed is maintained constant and is equal to 0.3 mm min^{-1} for all the tests. The fracture strength σ was evaluated according to the following relation [18]:

$$\sigma = \frac{3F_R}{2\pi h^2}\left[(1+\upsilon)\ln\frac{R_1}{R_2} + (1-\upsilon)(R_1^2 - R_0^2)/2R_2^2\right], \tag{1}$$

where F_R is the fracture force, υ is the Poisson's ratio of the glass, which is 0.22, h is the sample thickness which is considered as 3 mm and $R_0 = 8$ mm and $R_1 = 18$ mm are the radii of the inner and outer rings, respectively. If we use a square-shaped specimen with side length of $2L$, the equivalent radius must be inserted in the previous formulae as

$$R_2 = L(1+\sqrt{2})/2 \approx 1.21\,L, \tag{2}$$

where $2L$ is the squared sample side (50 mm).

3. Results and discussion

3.1 *Microscopic observations*

Figure 3 shows some details of the typical defects caused by three different grain sizes on the glass surface for sand mass $M_p = 120$ g. One can see clearly that the surface damage increases when the particle size is enhanced. So, this surface damage is proportional to the kinetic energy of particles. According to [19,20], the kinetic energy of sand grains is the most important factor governing the damage to glass by erosion. Consequently, the erosion phenomenon is more active in the case of large particles. After sandblasting tests, the surface state changes and the generated defects are distributed randomly over the entire surface. The surface damage is essentially produced by the interaction of defects and can be described as a progressive deterioration of the surface. The produced defects have various sizes and morphologies. In our study, we chose sand grains with irregular shapes. As a result, one can find such varieties of defects. For example, in the projected sand mass ($M_p = 120$ g), we admit that the size of the sand particles is the only parameter that affects the surface state.

3.2 *Erosion rate*

The samples used in sandblasting tests have various masses varying up to 120 g for three sizes of sand grains. One can notice that there is a gradual mass loss of the tested sample during sandblasting. Erosion rate is expressed as the ratio of sample mass losses Δm and projected sand masses M_p.

$$E = \Delta m / M_P. \tag{3}$$

The variation of erosion rate vs. projected sand masses for different grain sizes is illustrated in figure 4. The mass loss increases with increasing projected mass and grain size. It is well known that the kinetic energy of particles depends on the sand flux speed and the projected mass. In our case, the sand density of particles and the speed flux of each size are constant. As a result, the grain size is the only parameter that governs the kinetic energy. For larger grain size and higher kinetic energy, the surface damage becomes more important. Consequently, the surface roughness and mass loss increase, while the optical transmission and mechanical strength decrease. From figure 4, it can be observed that up to 100 g, the erosion rate decreases sharply with increasing sand masses and then tends towards a constant value for higher masses.

Grains size (μm)	Mp =120 g	Damage rate
300	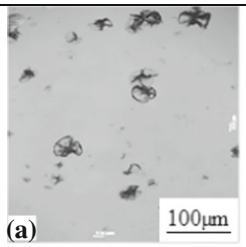	11.6 %
1000	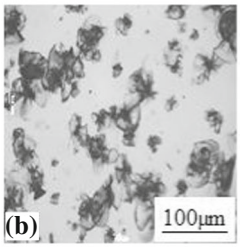	31.2 %
1700	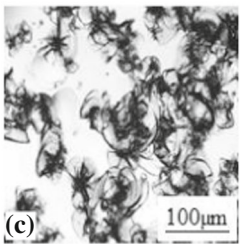	52.7 %

Figure 3. Typical erosion defects induced by sand projection of 120 g on glass for three grain sizes (300, 1000 and 1700 μm).

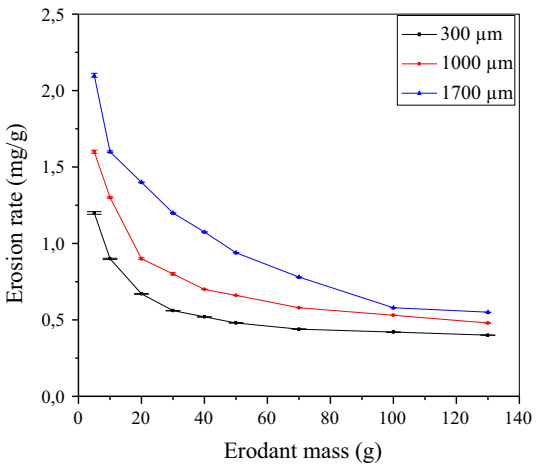

Figure 4. Variation of erosion rate with sand masses for three grains sizes (300, 1000 and 1700 μm).

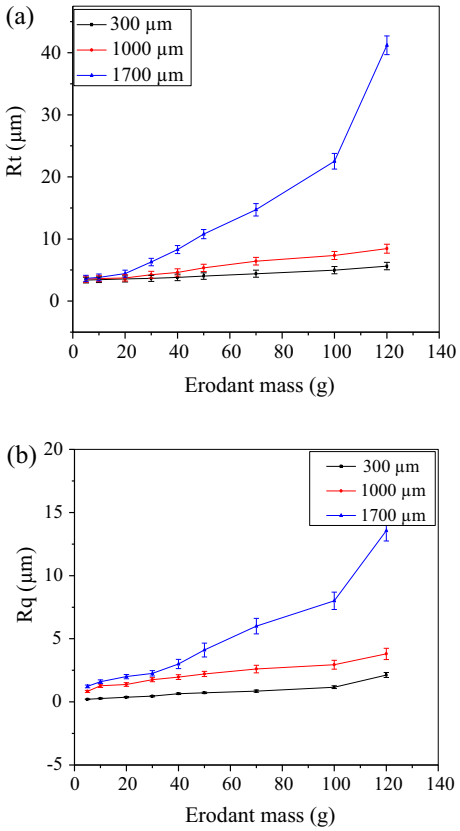

Figure 5. Variation of the root mean square roughness (R_q) and the total roughness R_t with sand masses for three grain sizes (300, 1000 and 1700 μm). (a) R_t and (b) R_q.

3.3 *Effect of mass and size of sand grains on the roughness*

Roughness is a parameter that characterises the surface state and reflects the damage rate of this surface exposed to erosion. The total roughness denotes the largest difference between the highest crest and the trough. This geometrical criterion is very important in the study of mechanical resistance. The quadratic roughness gives valuable information about optical quality. The variation of total and quadratic roughness as a function of projected sand mass for various grain sizes is plotted in figure 5. The roughness was measured in the central area of the samples, where it is most affected by erosion. We observe in figure 5a, a slight increase in roughness in the case of 300 and 1000 μm sand sizes for all projected masses. One can notice that the biggest size gives the highest values which reaches 41.2 μm for $M_p = 120$ g. The case of grain size ($\phi = 1700\,\mu$m) corresponds to a drastic decrease of the fracture strength for the highest projected masses. Figure 5b shows a slight increase of quadratic roughness, but the curve level is lower com-

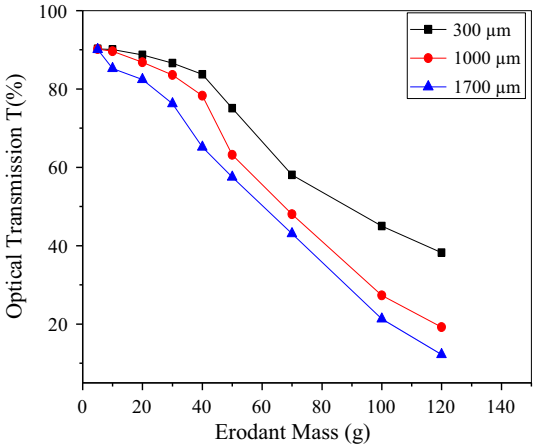

Figure 6. Variation of optical transmission $T(\%)$ with sand masses for three grains sizes (300, 1000 and 1700 μm).

pared to the values of total roughness. The highest value of quadratic roughness (13.7 μm) is obtained for the test conditions $M_p = 120$ g and $\Phi = 1700\,\mu$m. This value is higher if we look at the defect obtained by instrumented Vickers indentation.

3.4 *Optical transmission*

The measured optical transmission of the raw glass sample (not sandblasted) is 91.5%. For normal incidence, the optical transmission does not exceed 92%. These two glass sides cause a light loss of 4% by reflection. The particles' impact on glass surfaces generates various superficial defects such as microcracks, craters and scaling, which scatter the incident light and reduce the optical transmission. The variation of optical transmission vs. projected sand masses for various grain sizes is shown in figure 6. The optical transmission decreases when the sand masses increase, but the curve level depends on the grains' size. The kinetic energy involved becomes important for larger grain size and greater damage. When the eroded surface is not sufficiently damaged, the optical transmission loss is caused by reflection in small projected masses for the sandblasted states. For large projected masses, the decrease in the optical transmission is caused by light scattering. This result is similar to the result published by Benterki *et al* [6]. The lowest value of optical transmission reaches 12.24% when $M_p = 120$ g and $\phi = 1700\,\mu$m. The difference between these two extreme values can be explained by the importance of damage rate in the case of large grains. Also, the observed deviation between the curves can be due to the size and shape of the particles. The deviation of these two values explains that the effect of particle impact size on the glass surface is evident, but their shape effect is contestable. The sandblasting conditions and the results obtained are slightly different compared to the previous work, because of the nature of the sand, particle size and glass properties [21,22].

3.5 *Mechanical strength*

In this work, a ring-on-ring biaxial bending test was used. Among all bending tests, it appears that the ring-on-ring bending test is the most convenient and allows the elimination of the edge effect of the eroded samples. Also, the most damaged zone of the eroded sample (area under tension) coincides perfectly with the inner ring surface. Then, it can be assumed that the glass sample breaks due to the cracking initiated by the sand impact that covers the entire glass surface exposed to sandblasting. The ring-on-ring tests produce uniform bending zone and biaxial stresses are uniformly distributed over the eroded surface. Stuart [23] reported that during ring-on-ring biaxial bending, mechanical tests were performed on glass. As a result, a significant proportion of failures occur outside the inner ring and the failure does not necessarily occur at the location of the peak stress. Thus, our obtained resistance values are available since the damaged surface has a circular shape and is located in the central zone of the sample, which coincides with the inside diameter of the ring and the edges, that are not affected by sand impacts. The microscopic analysis of surface fracture shows that the failure extension is initiated from the central region of the sample, which is the most damaged area. This central region corresponds to the peak stress, where the critical crack most probably can be easily generated. The variation of the flexural strength vs. sand masses for three grain sizes is presented in figure 7. We remark that the mechanical strength decreases as the sand mass and grain size increase. For projected sand mass of 120 g and grain size of 1700 μm, the mechanical strength decreases considerably down to (9.56 ± 1.78) MPa. One can notice that the initial value is (117 ± 23) MPa. One explains this decrease by the increase of the total roughness and the high particle kinetic energy. In this context, Faci *et al* [17] have reported that the variations in mechanical strength evolve proportionally to the increase of the kinetic energy of the particles. The coarse particles are responsible for large defects accompanied by crack networks. The density of the surface defects increases following great number of impacts that can interact and lead to an increase in surface damage.

4. Conclusion

During sandblasting glass with different sand masses and grains sizes, there is a severe damage in the

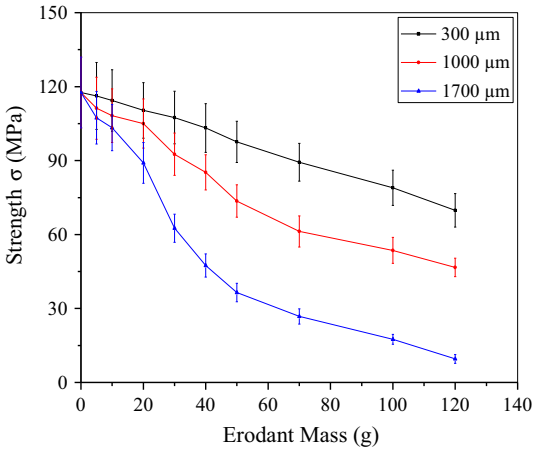

Figure 7. Variation of flexural strength with sand masses for three grains sizes (300, 1000 and 1700 μm).

sandblasted surface. The optical transmission and the mechanical strength decrease considerably as the projected sand masses increase, while the roughness increases. By varying the size of the grains, we notice a deterioration of the surface. This deterioration caused an increase in the surface roughness and a decrease in the optical transmission and mechanical strength. One can show that for $M_p = 120$ g and $\Phi = 1700\,\mu$m, both mechanical strength and optical transmission curves present minimum values of 9.56 MPa and 12.24% respectively. For this reason, the sand particles with a diameter of around 1700 μm produce crater-shaped defects on the eroded glass surface, the size of which is about 468 μm and the damage rate is 52.7%. The total roughness curve reaches the maximum value of 41.2 μm. In this case, severe flaws tend to cover the entire surface of the eroded specimen. Note that microscopic observations confirm our interpretations.

Acknowledgements

The authors acknowledge Taif University Research Supporting Project number (TURSP-2020/66), Taif University, Taif, Saudi Arabia.

References

[1] M Kolli, H Laouamri and N Bouaouadja, *Manuf. Sci. Tech.* **3(4)**, 114 (2015)
[2] A Ayadi, N Bouaouadja, A Duran and Y Castro, *Ceram. Int.* **46(8)**, 10634 (2020)
[3] B Barka, A Faci, N Bouaouadja, C Bousbaa, D Benachour and M Fatmi, *Int. J. Appl. Glass Sci.* **9(4)**, 471 (2018)
[4] S Benterki, A Faci and N Bouaouadja, *Int. J. Appl. Glass Sci.* **11(2)**, 245 (2020)
[5] S Benterki, N Laouar, C Bousbaa, N Bouras and N Bouaouadja, *Glass Technol*. **53(2)**, 53 (2012)
[6] S Benterki, C Bousbaa, N Laouar and A Faci, *Optik* **158**, 799 (2018)
[7] E M A Khalil, A Y Rasha, M Samer and M A Taha, *Ceram. Int.* **44(7)**, 7867 (2018)
[8] R A Youness, M A Taha, A El-Kheshen and M Ibrahim, *Ceram. Int*. **44(17)**, 20677 (2018)
[9] P Jha and K Singh, *Silicon.* **8(3)**, 437 (2015)
[10] M A Taha, A Rasha, R A Youness, G T El-Bassyouni and M A Azooz, *Silicon* **10(13)**, 3075 (2021)
[11] M A Ouis, M A Taha, G T El-Bassyouniand and M A Azooz, *Mater. Sci*. **10(42)**, 246 (2019)
[12] K Rompe and G Engel, *Soc. Automot. Eng. Tech. Paper* 840385 (1984)
[13] Q Fang, H Xu, P S Sidky and M G Hocking, *Wear* **224(2)**, 183 (1999)
[14] P J Slikkerveer, P C P Bouten and F C Haas, *Sensors Actuators A* **85(1–3)**, 296 (2000)
[15] ASTM G76-89, *Standard practice for conducting erosion tests by solid-particle impingement using gas jets* (ASTM, Philadelphia, 1992)
[16] ASTM C1499, Standard Test Method for Monotone Equibiaxial Flexural Strength of Advanced Ceramics at Ambient Temperature
[17] A Faci, S Benterki and N Bouaouadja, *J. Aust. Ceram. Soc*. **56**, 21 (2020)
[18]] M Kolli, M Hamidouche, N Bouaouadja and G Fantozzi, *J. Eur. Ceram. Soc.* **29(13)**, 2697 (2009)
[19] A G Evans, M E Gulden and M Rosenblatt, *Proc. R. Soc. Lond. Ser. A* **361(343)**, 1706 (1978)
[20] D B Marshall, B R Lawn and A G Evans, *J. Am. Ceram. Soc.* **65(11)**, 561 (1982)
[21] S Benterki, A Faci and C Bousbaa, *Silicon*, https://doi.org/10.1007/s12633-021-00991-y (2021)
[22] N Adjouadi, N Laouar, C Bousbaa, N Bouaouadja and G Fantozzi, *J. Eur. Ceram. Soc.* **27**, 3221 (2007)
[23] G Stuart Reid, *Civ. Eng. Environ. Syst.* **24(2)**, 139 (2007)